ANGULAR NEUTRON TRANSPORT INVESTIGATION IN THE HZETRN FREE-SPACE ION AND NUCLEON TRANSPORT AND SHIELDING COMPUTER PROGRAM

by

R.C. Singleterry
Engineering Division
Argonne National Laboratory
P. O. Box 2528
Idaho Falls, Idaho 83403-2528

and

J.W. Wilson
National Aeronautics and Space Administration
Langley Research Center, Mail Code 188B
Hampton, VA 23681-0001

Paper to be submitted for presentation at the
1997 Joint International Conference on Mathematical Methods
and Supercomputing for Nuclear Applications
Saratoga Springs, New York
October 6-10, 1997

Work supported by the U.S. Department of Energy, Reactor Systems, Development and Technology, under Contract W-31-109-Eng-38.

DISCLAIMER

Angular Neutron Transport Investigation in the HZETRN Free-Space Ion and Nucleon Transport and Shielding Computer Program

Robert C. Singleterry Jr.
Argonne National Laboratory – West
P.O. Box 2528
Idaho Falls, ID, USA 83403-2528
(208) 533 7879
singleterry@anl.gov

John W. Wilson
National Aeronautics and Space Administration
Langley Research Center, Mail Code 188B
Hampton, VA, USA 23681-0001
(757) 864 1414
JW_Wilson@qmgate.larc.nasa.gov

Abstract

Extension of the high charge and energy (HZE) transport computer program HZETRN for angular transport of neutrons is considered. For this paper, only light ion transport, He^4 and lighter, will be analyzed using a pure solar proton source. The angular transport calculator is the ANISN/PC program which is being controlled by the HZETRN program. The neutron flux values are compared for straight-ahead transport and angular transport in one dimension. The shield material is aluminum and the target material is water. The thickness of these materials is varied; however, only the largest model calculated is reported which is $50\frac{gm}{cm^2}$ of aluminum and $100\frac{gm}{cm^2}$ of water. The flux from the ANISN/PC calculation is about two orders of magnitude lower than the flux from HZETRN for very low energy neutrons. It is only a magnitude lower for the neutrons in the 10 to 20 MeV range in the aluminum and two orders lower in the water. The major reason for this difference is in the transport modes: straight-ahead versus angular. The angular treatment allows a longer path length than the straight-ahead approximation. Another reason is the different cross section sets used by the ANISN/PC-BUGLE-80 mode and the HZETRN mode. The next step is to investigate further the differences between the two codes and isolate the differences to just the angular versus straight-ahead transport mode. Then, create a better coupling between the angular neutron transport and the charged particle transport.

I. INTRODUCTION

The prediction of harm from radiation in free-space environments is an important subject for future space travel with humans or sophisticated robots and for current travel with automated systems. Their functioning over time is dependent on the damage caused by the environment they inhabit. The accurate prediction of radiation levels in this environment is the first step in the determination of damage.

During the last 40 years, propagation of space radiation through matter has been the subject of many studies. Reference [1] outlines the major studies and their results. The conclusion of these studies is that the process is well understood but a complete compact solution is still elusive. Stochastic methods such as Monte Carlo can be used to determine the dose field of interest, but not in a timely manner to enable optimization of shielding for design analysis. Therefore, deterministic methods are being developed. The most advance system so far is the HZETRN program developed by one of us (J.W. Wilson) and others that executes under a VMS computer environment and is discussed in Reference [1]. It predicts dose fields in simulated tissue behind a shield in spherical coordinates for high-charge-and-energy particles. Many simplifying assumptions that do not impact the final solution have been used. It also uses a few simplifying assumptions in which the impacts are unknown. This analysis extends the current flux predictions in HZETRN by exchanging the straight-ahead transport of evaporation neutrons with angular transport. From this we can determine whether this method exchange make neutrons a more important contributor to the dose and outline where the next upgrade effort should be focused.

The approach for this analysis is the creation of an isotropic source of evaporation neutrons in HZETRN for use in the ANISN/PC neutral particle transport solver. This decouples the transport of the neutrons from the larger system, but is the first step to a coupled model and will at least determine if the angular neutron transport component is important. The ANISN/PC program was chosen because of its long history and current implementation in a PC environment with source code (Reference [2]). One of us (R.C. Singleterry Jr.) converted it to execute under a VMS computer environment and extended its memory size to handle large problems.

The current state of this analysis is the prediction and comparison of the neutron flux components between the straight-ahead and angular models. Only the light ions, He^4 and lighter, are considered. The initial source of protons is the solar particle event of August 1972 with King's fitting. Later implementations will consider heavy galactic cosmic ions and different particle sources, plus calculate doses associated with the neutron flux calculated by the angular method.

This paper describes the work involved with modifying the HZETRN program and the creation of a source generator for ANISN/PC. Section II. describes the transport phenomena occurring and the solution methods used. Section III. describes how the HZETRN and ANISN/PC codes were coupled. Sections IV. and V. show the results obtained and discusses these results in light of the problem being solved. Finally, Section VI. draws conclusions from this analysis and describes where to go next.

II. Transport Phenomena and Solutions

Various collision events occur in this physical system. When the ion enters a material, the electron clouds interact over a long range with the ion. These interactions are characterized by a low exchange of energy per event. If an ion's path encounters an atom's nucleus, then large energy exchange events occur. The descriptions below outline what Boltzmann transport equations are relevant in this problem and how the programs solve the equations.

A. Boltzmann Equation and Solution for HZETRN Light Ions

A complete description of the derivation and solution method for HZE ions can be found in Reference [1]. A short overview is repeated here for completeness. The initial equation starts with a heuristic derivation from particle conservation principles in an elemental sphere of radius δ

$$\begin{aligned}\phi_j(\vec{r}+\delta\vec{\Omega},\vec{\Omega},\mathrm{E})\ \delta^2\ \mathrm{d}\vec{\Omega} \ &= \ \phi_j(\vec{r}-\delta\vec{\Omega},\vec{\Omega},\mathrm{E})\ \delta^2\ \mathrm{d}\vec{\Omega}\ + \\ &+ \ \delta^2\ \mathrm{d}\vec{\Omega}\int_{-\delta}^{+\delta}\mathrm{d}l\sum_k\int\mathrm{d}\vec{\Omega}'\int\mathrm{dE}'\ \sigma_{jk}(\vec{\Omega},\vec{\Omega}',\mathrm{E},\mathrm{E}')\ \phi_k(\vec{r}+l\vec{\Omega},\vec{\Omega}',\mathrm{E}')\ - \\ &- \ \delta^2\ \mathrm{d}\vec{\Omega}\int_{-\delta}^{+\delta}\mathrm{d}l\ \sigma_j(\mathrm{E})\ \phi_j(\vec{r}+l\vec{\Omega},\vec{\Omega},\mathrm{E}) \end{aligned} \tag{1}$$

where,

$\phi_j(\vec{r}+\delta\vec{\Omega},\vec{\Omega},\mathrm{E})\ \delta^2\ \mathrm{d}\vec{\Omega}$ represents the flux of type j particles leaving a surface element $\delta^2\vec{\Omega}$ on a sphere,

$\phi_j(\vec{r}-\delta\vec{\Omega},\vec{\Omega},\mathrm{E})\ \delta^2\ \mathrm{d}\vec{\Omega}$ represents the flux of type j particles entering the surface element,

$\delta^2\ \mathrm{d}\vec{\Omega}\ \int_{-\delta}^{+\delta}\mathrm{d}l\ \sum_k\ \int\mathrm{d}\vec{\Omega}'\ \int\mathrm{dE}'\ \sigma_{jk}(\vec{\Omega},\vec{\Omega}',\mathrm{E},\mathrm{E}')\ \phi_k(\vec{r}+l\vec{\Omega},\vec{\Omega}',\mathrm{E}')$ represents the source of type j particles from atomic and nuclear collisions,

$\delta^2\ \mathrm{d}\vec{\Omega}\ \int_{-\delta}^{+\delta}\mathrm{d}l\ \sigma_j(\mathrm{E})\ \phi_j(\vec{r}+l\vec{\Omega},\vec{\Omega},\mathrm{E})$ represents the losses to atomic and nuclear collisions,

$\phi_j(\vec{r}, \vec{\Omega}, E)$ represents the flux of type j particles at point $\vec{r}$, moving in direction $\vec{\Omega}$, with energy E,

$\sigma_{jk}(\vec{\Omega}, \vec{\Omega}', E, E')$ represents the macroscopic cross section for a particle of type k moving in direction $\vec{\Omega}'$ and with energy E′ appears as particle of type j moving in direction $\vec{\Omega}$ with energy E after an interaction, and

$\sigma_j(E)$ represents the total macroscopic cross section of interaction.

If equation (1) is expanded about δ and terms to order δ^3 are kept, then the time-independent form of the Boltzmann transport equation for dual-species tenuous gas is generated by dividing by the cylindrical volume $2\delta\left(\delta^2 d\vec{\Omega}\right)$

$$\vec{\Omega} \cdot \nabla\phi_j(\vec{r}, \vec{\Omega}, E) \;=\; \sum_k \int d\vec{\Omega}' \int dE' \; \sigma_{jk}(\vec{\Omega}, \vec{\Omega}', E, E') \; \phi_k(\vec{r}, \vec{\Omega}', E') \;-\; \sigma_j(E) \; \phi_j(\vec{r}, \vec{\Omega}, E). \tag{2}$$

The particle creation and loss cross sections, $\sigma_{jk}(\vec{\Omega}, \vec{\Omega}', E, E')$ and $\sigma_j(E)$, can be separated into their atomic and nuclear interaction constituents. Concentrating on the atomic component only, the differential cross section can be approximated by

$$\sigma_{jk}^{\mathrm{at}}(\vec{\Omega}, \vec{\Omega}', E, E') \;\approx\; \sum_n \sigma_j^{\mathrm{at}}(E')\delta\left(\vec{\Omega} \cdot \vec{\Omega}' - 1\right) \; \delta_{jk} \; \delta\left(E + \epsilon_n - E'\right) \tag{3}$$

where ϵ_n represents the excitation energy corresponding to the electron excitation level n. The atomic cross sections can then be approximated by

$$\begin{aligned}
&\sum_k \int d\vec{\Omega}' \int dE' \; \sigma_{jk}^{\mathrm{at}}(\vec{\Omega}, \vec{\Omega}', E, E') \; \phi_k(\vec{r}, \vec{\Omega}', E') \;-\; \sigma_j^{\mathrm{at}}(E) \; \phi_j(\vec{r}, \vec{\Omega}, E) \;= \\
&= \sum_n \sigma_{jn}^{\mathrm{at}}(E + \epsilon_n) \; \phi_j(\vec{r}, \vec{\Omega}, E + \epsilon_n) \;-\; \sigma_j^{\mathrm{at}}(E) \; \phi_j(\vec{r}, \vec{\Omega}, E) \\
&\approx \sum_n \sigma_j^{\mathrm{at}}(E) \; \phi_j(\vec{r}, \vec{\Omega}, E) \;+\; \sum_n \epsilon_n \frac{\partial}{\partial E}\left[\sigma_{jn}^{\mathrm{at}}(E) \; \phi_j(\vec{r}, \vec{\Omega}, E)\right] \;-\; \sigma_j^{\mathrm{at}}(E) \; \phi_j(\vec{r}, \vec{\Omega}, E) \\
&= \frac{\partial}{\partial E}\left[S_j(E) \; \phi_j(\vec{r}, \vec{\Omega}, E)\right]
\end{aligned} \tag{4}$$

where

$$\sigma_j^{\mathrm{at}}(E) \;=\; \sum_n \sigma_{jn}^{\mathrm{at}}(E),$$

and

$$S_j(E) \;=\; \sum_n \sigma_{jn}^{\mathrm{at}}(E) \; \epsilon_n.$$

Using equation (4) in equation (3), the usual continuous slowing-down approximation is created

$$\left[\vec{\Omega} \cdot \nabla \;-\; \frac{1}{A_j}\frac{\partial}{\partial E}S_j(E) \;+\; \sigma_j(E)\right] \; \phi_j(\vec{r}, \vec{\Omega}, E) \;=\; \sum_k \int d\vec{\Omega}' \int dE' \; \sigma_{jk}(\vec{\Omega}, \vec{\Omega}', E, E') \; \phi_k(\vec{r}, \vec{\Omega}', E') \tag{5}$$

where

$\phi_j(\vec{r}, \vec{\Omega}, E)$ represents the flux of type j particles with atomic mass A_j at $\vec{r}$, moving in direction $\vec{\Omega}$ with energy E measured in units of A MeV,

$S_j(E)$ represents the linear energy transfer (LET),

$\sigma_j(E)$ represents the total macroscopic cross section of nuclear interaction, and

$\sigma_{jk}(\vec{\Omega}, \vec{\Omega}', \mathrm{E}, \mathrm{E}')$ represents the production cross section for type j particles with energy E and moving in direction $\vec{\Omega}$ by collision of type k particles with energy E$'$ and moving in direction $\vec{\Omega}'$.

Therefore, all cross sections in equation (5) are for nuclear interactions only.

A known flux for each particle type must be defined on the boundary to complete the solution

$$\phi_j(\vec{\Gamma}, \vec{\Omega}, \mathrm{E}) = f_j(\vec{\Gamma}, \vec{\Omega}, \mathrm{E})$$

where

$$\vec{\Omega} \cdot \vec{n}(\vec{\Gamma}) < 0$$

and $\vec{n}(\vec{\Gamma})$ is the outward directed normal to the boundary surface at point $\vec{\Gamma}$.

Without going into the mathematical details, various simplifications can be made for the particle source term in equation (5). The fragmentation of target nuclei can be ignored if the particle energy is large in comparison to the momentum spread of the secondary particles created by the interaction. Space radiations, being nearly isotopic and forward-peaked in spectrum, allow the straight-ahead approximation for a description of the transport of charged particles and high energy neutrons. HZETRN also uses this same approximation to transport low energy neutrons which is not a valid approximation for these conditions. Once these approximations are incorporated into equation (5), for light ions and high energy neutrons, it reduces to

$$\left[\frac{\partial}{\partial x} - \frac{\partial}{\partial \mathrm{E}}\tilde{S}_j(\mathrm{E}) + \sigma_j(\mathrm{E})\right] \phi_j(x, \mathrm{E}) = \sum_k \int_{\mathrm{E}}^{\infty} \mathrm{dE}'\, m_{jk}(\mathrm{E}, \mathrm{E}')\, \sigma_k(\mathrm{E}')\, \phi_k(x, \mathrm{E}'), \qquad (6)$$

where

$\phi_j(x, \mathrm{E})$ represents the flux of particles of type j with atomic mass A_j at x moving along the X-axis at energy E in units of A MeV,

$\sigma_j(\mathrm{E})$ represents the macroscopic nuclear absorption cross section,

$\tilde{S}_j(\mathrm{E})$ represents the change in E per unit distance, and

$m_{jk}(\mathrm{E}, \mathrm{E}')$ represents the multiplicity of ion type j produced by ion type k in a collision.

To solve equation (6), coordinate transforms are matched with a flux transform to create an one-dimensional differential equation which is solved by using line integration with an integrating factor. The coordinate transforms are

$$\eta_j \equiv x - R_j(\mathrm{E})$$

and

$$\xi_j \equiv x + R_j(\mathrm{E}).$$

The flux transform is

$$\chi_j(\eta_j, \xi_j) \equiv \tilde{S}_j(\mathrm{E})\, \phi_j(x, \mathrm{E}) = \psi_j(x, r_j),$$

where

$$r_j = \int_0^{\mathrm{E}} \frac{\mathrm{dE}'}{\tilde{S}_j(\mathrm{E}')}.$$

With these definitions, a flux propagation technique along the X-axis is generated

$$\psi_j(x+h, r) = e^{-\sigma_j(r)h}\psi_j(x, r+\nu_j h) + \sum_i \int_{r+\frac{1}{2}\nu_j}^{\infty} \mathrm{d}r'\, \psi_i(x, r' + \frac{1}{2}\nu_j) \int_0^h \mathrm{d}z' e^{-\sigma_j(r)h} \bar{f}_{ji}(r+\nu_j z, r'),$$

where r is the proton residual range (Reference [3]). An error and truncation analysis along with various numerical techniques are included in the program to increase accuracy.

B. Boltzmann Equation and Solution for Neutral Particle Transport

The form of the Boltzmann transport equation described in the last section is not valid for low energy neutrons. The straight-ahead approximation does not allow for hard-sphere scattering collisions that result in a change of direction of these neutrons. In some materials, this reaction type is very important. This is especially true for low energy neutrons which also can disproportionately contribute to the dose rate.

The Boltzmann transport equation of interest for the low energy neutron environment is the time-independent, multiple energy group, anisotropic scattering, neutral particle transport equation. This is generated from the time-independent continuous equation (Reference [4])

$$\vec{\Omega} \cdot \nabla \, \phi(\vec{r}, \vec{\Omega}, E) \; + \; \sigma_t(\vec{r}, E) \, \phi(\vec{r}, \vec{\Omega}, E) \; = \\ = \int_0^\infty dE' \int_{-1}^{+1} d\vec{\Omega}' \left[\chi(E) \, \nu \, \sigma_f(\vec{r}, E') \; + \; \sigma_s(\vec{r}, \vec{\Omega}' \to \vec{\Omega}, E' \to E) \right] \phi(\vec{r}, \vec{\Omega}', E') \; + \; Q(\vec{r}, \vec{\Omega}, E), \tag{7}$$

where

$\phi(\vec{r}, \vec{\Omega}, E)$ represents the particle flux,

$\sigma_t(\vec{r}, E)$ represents the total nuclear interaction probability,

$\nu \, \sigma_f(\vec{r}, E')$ represents the number of neutrons generated after a fission event,

$\chi(E)$ represents the fission neutron spectrum,

$\sigma_s(\vec{r}, \vec{\Omega}' \to \vec{\Omega}, E' \to E)$ represents the source of neutrons from other energies and directions after a scattering event, and

$Q(\vec{r}, \vec{\Omega}, E)$ represents an external source of neutrons which for this paper will be the evaporation neutron source from the HZETRN code.

This equation is then discretized in energy, angle, and space. Reference [5] gives a complete derivation, but a short derivation is given here for completeness.

The energy domain is discretized into G number of energy groups and equation (7) is integrated over these groups to obtain

$$\vec{\Omega} \cdot \nabla \phi_g(\vec{r}, \vec{\Omega}) \; + \; \sigma_g^t(\vec{r}) \, \phi_g(\vec{r}, \vec{\Omega}) \; = \\ = \sum_{g'=1}^{G} \int_{-1}^{+1} d\vec{\Omega}' \left[\chi_g \, \nu \, \sigma_{g'}^f(\vec{r}) \; + \; \sigma_{g' \to g}^s(\vec{r}, \vec{\Omega}' \to \vec{\Omega}) \right] \phi_{g'}(\vec{r}, \vec{\Omega}') \; + \; Q_g(\vec{r}, \vec{\Omega}) \tag{8}$$

for $g = 1, \ldots, G$. The energy-averaged group cross sections formulations can be found in numerous text books (Reference [4] for example). These energy groups can also include multiple neutral particle types. The main purpose for this is neutron/gamma particle transport for shielding calculations.

The scattering cross section needs special treatment because it measures a change in direction and energy. The usual treatment is to expand this cross section in orthogonal polynomials about direction μ; in the case, Legendre polynomials are used. To represent the cross section values exactly, an infinite number of polynomials are needed; however, the usual procedure is to truncate the number to L which is less than 10 for normal materials. The next step is to discretize the angular variable into M directions. This creates a problem in the scattering cross section term because it resides inside an integral. The usual procedure is to choose angles that coincide with some quadrature integration scheme dependent on the number of dimensions in the problem. For the one dimensional slab or spherical ANISN/PC program, the gauss quadrature scheme is usually used. These manipulations are applied to equation (8) to obtain

$$\mu^m \cdot \nabla\, \phi_g^m(\vec{r}) \;+\; \sigma_g^t(\vec{r})\, \phi_g^m(\vec{r}) \;=\; \sum_{g'=1}^{G} \left[\chi_g\, \nu\, \sigma_{g'}^f(\vec{r})\, \phi_g^0(\vec{r})\right] \;+$$

$$+\; \sum_{g'=1}^{G} \sum_{l=0}^{L} \left[(2l+1)\, P_l(\mu^m)\, \sigma_{g'\to g}^{sm}(\vec{r}) \sum_{m'=0}^{M} w^{m'}\, P_l(\mu^{m'})\, \phi_g^{m'}(\vec{r})\right] \;+\; Q_g^m(\vec{r}) \tag{9}$$

for $g = 1, \ldots, G$ and $m = 1, \ldots, M$. The weights and directions can be any arbitrary value, but to ensure proper and consistent integration with known physics, these rules should be followed

$$\sum_{m=1}^{M} w^m \;=\; 1.0,$$

$$\sum_{m=1}^{M} [(\mu^m)^n\; w^m] \;=\; 0 \qquad\qquad n \;=\; \text{odd},$$

and

$$\sum_{m=1}^{M} [(\mu^m)^n\; w^m] \;=\; \frac{1}{n+1} \qquad\qquad n \;=\; \text{even}.$$

To complete the basis of this solution method, finite differences is used to discretize the spatial variable. Therefore, only flux values at specific points in the space, angle, and energy domains are calculated. In one dimension

$$\mu^m \left[\frac{\phi_g^m(x_{i+\frac{1}{2}}) \;-\; \phi_g^m(x_{i-\frac{1}{2}})}{\Delta x_i}\right] \;+\; \sigma_g^t(x_i)\, \phi_g^m(x_i) \;=\; \sum_{g'=1}^{G} \left[\chi_g\, \nu\, \sigma_{g'}^f(x_i)\, \phi_{g'}^0(x_i)\right] \;+$$

$$+\; \sum_{g'=1}^{G} \sum_{l=0}^{L} \left[(2l+1)\, P_l(\mu^m)\, \sigma_{g'\to g}^{sm}(x_i) \sum_{m'=0}^{M} w^{m'}\, P_l(\mu^{m'})\, \phi_{g'}^{m'}(x_i)\right] \;+\; Q_g^m(x_i) \tag{10}$$

for $g = 1, \ldots, G$, $m = 1, \ldots, M$, and $i = 1, \ldots, I$, where I is the number of mesh nodes. With this formulation, two unknowns exist: $\phi_g^m(x_{i+\frac{1}{2}})$ and $\phi_g^m(x_i)$. The value for $\phi_g^m(x_{i-\frac{1}{2}})$ was found in the $i-1$ node calculation or is a boundary condition. Since two unknowns exist, another equation besides equation (10) is needed. The second equation represents the transport of the particles through mesh cell i. Various schemes have been used; however, the diamond differencing scheme is the most popular. Its form is

$$\phi_g^m(x_i) \;=\; \frac{1}{2}\left[\phi_g^m(x_{i+\frac{1}{2}}) \;+\; \phi_g^m(x_{i-\frac{1}{2}})\right]$$

or just the arithmetic average of the flux over the width of the mesh cell.

To complete the neutral particle solution, an iteration or propagation scheme is needed. For the complexity in equation (10), two iterations are employed. The first or outer iteration is over the fission source since this source is a function of the flux. The second or inner iteration is over the mesh, angular, and group structure using the source terms (including scatter and external sources) from the latest outer iteration. This continues until the values from the previous iteration are within a user selected tolerance to the current iteration. Other schemes to accelerate these iterations are employed, but the details are not necessary to complete this overview. In the HZETRN circumstances, the outer iteration is not used because a fission process does not exist.

The discrete ordinates solution scheme has been used for many years to solve complex problems of neutral particle transport. It is a proven method that is stable in execution within certain known limitations. These attributes along with ANISN/PC's own history are why this particular solution was chosen. Other solution methods such as F_N are also being investigated and will probably replace ANISN/PC due to CPU time and disk space limitations.

III. Combining the HZETRN and ANISN/PC Programs

To improve upon the HZETRN straight-ahead model for neutrons, the creation of neutrons must be separated from the transport process and stored. The major source of neutrons is the evaporation neutrons *boiling off* the nuclei after a high energy collision. These neutrons are gathered by the energy groups used in ANISN/PC and fed into the code. The control of this new transport mode is handled in HZETRN for future expansion in the coupled environment.

The neutrons are generated by collisions of the primary ions and their secondaries with nuclei of the shield material or in the tissues of the astronaut. The present neutron production spectra are those calculated by the Bertini code which is the cross section database of the HETC code and remains an option in the Los Alamos version of HETC (LAHET). The resulting cross sections are given in terms of a cascade spectrum produced by the direct action of the colliding particle and an evaporation spectrum in the final deexcitation of the residual nucleus.

In the present calculation, we run the HZETRN code with the evaporation contributions removed which allows us to evaluate the cascade produced particle fields. The evaporation source spectra are then evaluated explicitly as a function of the collisions of the cascade fields and provide the low energy source terms for the ANISN code. We assume the evaporation neutron source to be isotropic. The difference between the cascade fields and the full HZETRN solution is taken as the evaporation fields calculated by the HZETRN code.

The isotropic neutron source is now stored by energy group and position. The spatial mesh used by the HZETRN code is changed to conform to stability requirements needed by the discrete ordinates method (mesh size no larger than one-half of the minimum mean free path length). A linear interpolation is performed between HZETRN mesh points to fill in the ANISN/PC source array. An ANISN/PC input deck is written for an S_8 calculation in spherical geometry with two regions. The first or outside region is the shield, aluminum in this paper. The second region is the target or water. A call to the VMS routine LIB$SPAWN executes ANISN/PC and creates a punch file that contains the scalar flux. The punch file is then read and the flux values are collapsed to the original HZETRN energy grouping and output for comparison to HZETRN.

The cross sections used by the HZETRN code are described in detail in References [1], [6], and [7] and will not be discussed here. The ANISN/PC cross section set is BUGLE-80 (Reference [8]). This is a coupled neutron/gamma, P_3 cross section set designed for pressurized water reactor shielding problems. While this data set is not designed or optimized for this problem, it can give order of magnitude type results for comparison purposes. Better and specialized data sets are being sought to extend the energy range of applicability and better match the flux source. The next step is to force HZETRN to use the same cross section set as ANISN/PC to enable the detection of pure transport differences instead of the mixed transport/cross section differences identified in this paper.

IV. Results

The model used to generate results for this paper has the aluminum shield with a maximum thickness of 50 $\frac{g}{cm^2}$ while the water target has a maximum thickness of 100 $\frac{g}{cm^2}$. With the straight-ahead approximation, the nodes already calculated do not depend on the current node being calculated. Therefore, once a node is calculated, it is a valid node for every subsequent calculation. This is not the case for the ANISN/PC executions. Each node layout is an independent calculation and cannot be used for future calculations. Therefore, separate ANISN/PC calculations are needed for every combination of material thicknesses used in HZETRN.

After a nominal execution of the HZETRN code is performed for pure straight-ahead transport, another run is executed using the ANISN/PC code to transport the evaporation neutrons. The residual straight-ahead neutron flux from the ANISN/PC run is subtracted from the nominal run to isolate the distribution of evaporation neutrons transported by the straight-ahead propagation. This is then compared to the flux distribution calculated by ANISN/PC.

Only the nine lowest energy groups from HZETRN produce values below the 20 MeV limit of the BUGLE-80 cross sections. To save space in this paper, only the results from the largest model are shown in Figures 1 and 2. Figure 1 shows the flux values for the first five energy groups. These are the *lowest* in absolute energy which is different than the group structure in BUGLE-80 and that commonly encountered in Nuclear Engineering. Figure 2 shows the flux values for the next four energy groups. Table 1 shows the layout of the energy groups.

V. Discussion of Results

There is a marked reduction in the neutron particle flux when ANISN/PC is used as the transport solver. The reduction for low energy neutrons (energies below 2 MeV) is two orders of magnitude. For higher energy neutrons (2 to 20 MeV), the difference is much less. There are at least two explanations for this difference. The first involves the different cross section sets being used to transport the neutrons through the media. The HZETRN cross sections are coarse, unrefined, and based on the theory of and curve fits to interaction processes. The BUGLE-80 cross sections are obtained from experimental data and are highly accurate for the situation of pressurized water reactor shielding. It is unknown whether this problem is reducing or increasing the flux values at this time. The second reason involves the increase in total path length of the neutron by the scattering process. This allows more of a chance for neutrons to interact with media nuclei. The straight-ahead approximation uses the shortest possible path to transport the neutron through the media. This added path length and the added interactions will tend to decrease the flux values at a particular energy and spread them over all energies.

Both of these problems can be better quantified to some extent. If the HZETRN code is modified to accept the total cross section being utilized in the ANISN/PC code, then the same interaction probabilities are predicted for both codes and the difference from this aspect would just be from the scattering process. The second part is somewhat harder to quantify. As a first step, the number of angular bins can be reduced from 8 to 2 for a better simulation of the straight-ahead approximation. Then, it can be increased to 32 or higher to determine the importance of scattering to the problem. It is unclear at this time what results might be expected from this analysis. Other minor model adjustments can also be made to better simulate the results from HZETRN and close flux gap seen in this paper. These problems are being studied and will be reported on in the future.

VI. Conclusions

A more realistic low energy neutron transport method was investigated for the HZETRN computer code. It showed the expected result of a lowering of the neutron flux throughout the system. Two competing reasons to explain the reduction were identified and will be investigated in the future. The first involves the different cross section sets used by the HZETRN and the ANISN/PC codes. If the same set was used in both codes, it is unclear whether the flux would increase or decrease. The second involves the lengthening of the neutron's path through the media due to the scattering process which increases the probability of a neutron interacting with the media. Due to the nature of the new neutron transport method, significant revision of the HZETRN code is needed to incorporate neutrons in the dose calculation and these results will be reported in the future.

This appears to be a promising area of research to better understand what radiation fields exist in the space between planets. These methods can also be utilized in other aspects of space radiations which include low earth orbit and high altitude aircraft. The better we understand space radiation fields, the better the designs for protection are, and ultimately, the protection measures will be less expensive per unit of protection.

References

[1] Wilson, J.W., et al.; **HZETRN: Description of a Free-Space Ion and Nucleon Transport and Shieling Computer Program**, NASA Technical Paper 3495, May 1995.

[2] Parsons, D.K.; **ANISN/PC Manual**, EGG-2500, December 1988.

[3] Lamkin, S.L., et. al; *Space Proton Transport in One-Dimension*, **Nuclear Science and Engineering**, Vol 116, pgs. 291-299, 1994.

[4] Bell, G.I., Glasstone, S.; **Nuclear Reactor Theory**, Robert E. Krieger Company, 1970.

[5] O'Dell, R.D., Alcouffe, R.; **Transport Calculations for Nuclear Analysis: Theory and Guidelines for Effective Use of Transport Codes**, LA-10983-MS, Los Alamos National Laboratory, September 1987 (available on the Los Alamos publications Web Page).

[6] Wilson, J.W., et al.; **A Hierarchy of Transport Approximations for High Energy Heavy (HZE) Ions**, NASA Technical Memo TM-4118, 1989.

[7] Wilson, J.W., et al.; **BRYNTRN: A Baryon Transport Model**, NASA Technical Paper TP-2887, 1989.

[8] Roussin, R.W.; **RSIC Data Library Collection: BUGLE-80**, Oak Ridge National Laboratory, RSIC, DLC-75, 1980.

Table 1: Layout of Energy Groups Reported in Figures 1 and 2

Energy Group	Maximum Group Energy (MeV)
1	1.000E-02
2	7.050E-02
3	0.256
4	0.674
5	1.542
6	3.265
7	6.698
8	13.475
9	20.334

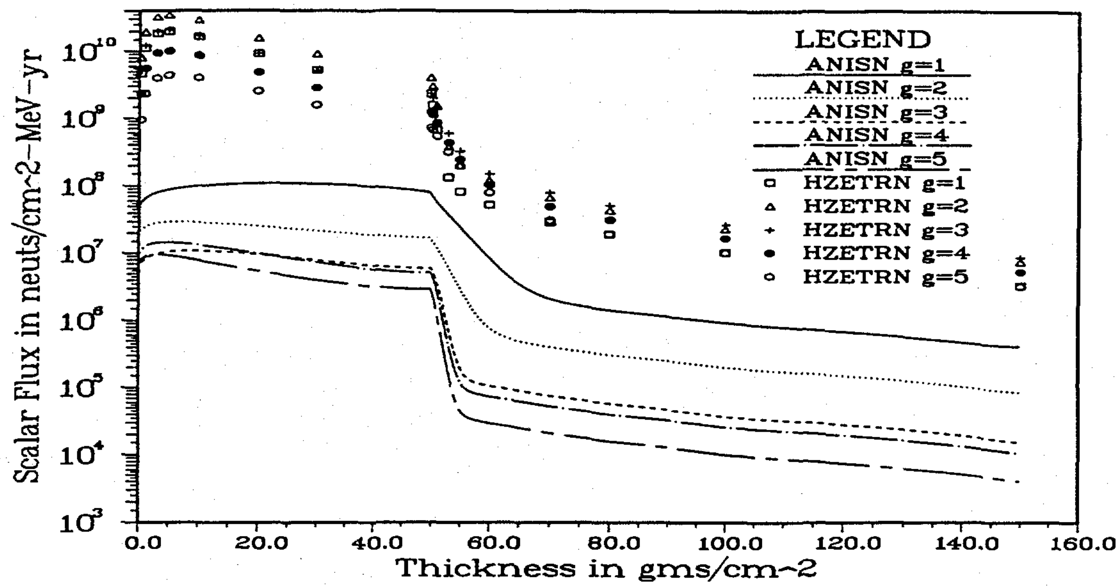

Figure 1: Neutron Flux Plot Comparisons for Energy Groups 1 through 5 Between HZETRN and ANISN

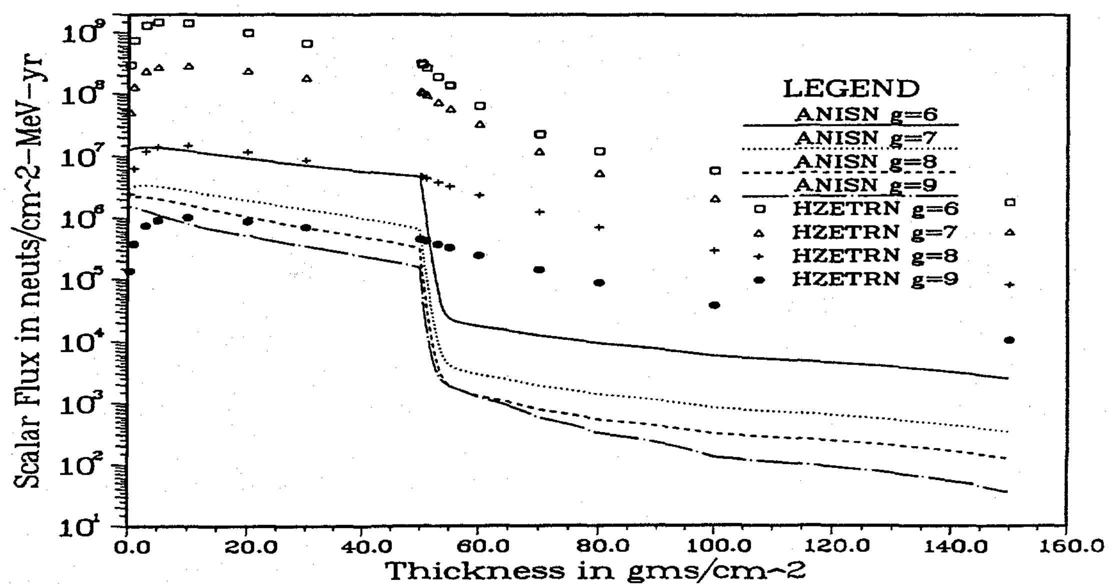

Figure 2: Neutron Flux Plot Comparisons for Energy Groups 6 through 9 Between HZETRN and ANISN